AUT Journal of Modeling and Simulation

AUT J. Model. Simul., 55(1) (2023) 171-182
DOI: 10.22060/miscj.2023.22482.5326

Neural Network based Fault Tolerant LQR Control for Orbital Maneuvering in LEO Satellites using Hall Effect Thrusters

E. Jahanbazi goujani, F. Jahangiri*, M. R. Mohammadi Damabi

Department of Electrical Engineering, Shahid Beheshti University, Tehran, Iran

ABSTRACT: This paper develops a neural network-based fault tolerant LQR control for orbital maneuvering of satellites in low altitude orbit that are subjected to disturbances like earth gravity, atmospheric drag, third body, and solar radiation. The controller is also developed such that it tolerates the effects of additive and effective loss of actuator faults. A neural network is used in the controller to estimate disturbances and faults and decrease their effects. Due to the high efficiency of electric thrusters, they are used widely in LEO (Low Earth Orbit) missions. Therefore, in this paper Hall effect thrusters are used as the actuator. For the maneuvering purpose, the reference orbit parameters are derived from a reference orbital dynamics which is the Kepler dynamics subjected to only the disturbance of gravity. To avoid singularity, the orbital dynamics of six modified elements are used in the control design besides the six classical elements. Then, by the desired orbital parameters from the reference orbit, the relative motion elements are calculated to apply in control laws. By Lyapunov analysis, the updating laws of the weights of the control and neural network are derived and also ultimately boundedness of the error between the nominal orbital elements and the faulty orbital elements is proved. To show the effectiveness of the proposed control, it is applied in the nonlinear Kepler dynamics which is affected by an accurate model of natural disturbances.

Review History:

Received: Jun. 16, 2023
Revised: Aug. 13, 2023
Accepted: Oct. 07, 2023
Available Online: Oct. 10, 2023

Keywords:

Modified orbital elements
Hall effect thrusters
orbital maneuvering
Neural network fault tolerant LQR control
orbital disturbances

1- Introduction

Orbital maneuvers have a significant role in the success of missions like surveillance, tracking, and data acquisition. The classical maneuvering approach applies a two-impulse Hohmann transfer to place the satellite in the correct orbital position [1]. Despite the fuel efficiency of this control method, it is inherently an open loop, and also an approximation of the impulsive thrust is required. To overcome these limitations and also due to the requirements of more accurate positioning in next-generation space missions, considerable researches are focused on the development of feedback control systems. Specially since new continuous thrust propulsion technologies are available to apply the continuous control commands [2, 3].

The design of feedback controllers like Lyapunov based methods are able to control orbital maneuvering with stability guaranteeing [4-8]. Unlike providing analytical control laws, this method generally does not minimize a predefined maneuver cost. Since minimizing fuel consumption along with precise maneuvering is very significant in spacecraft missions, optimal controls have been largely used to solve the problem [9-14]. In [13-16], MPC is used to solve an optimal maneuvering problem. However, this technique is usually computationally intensive, especially when the dynamics are nonlinear, as it requires to solve LMIs at each time step. decreased the difficulties by performing linearization in a curvilinear coordinate system. However, this approach is limited by the assumption of a small relative radius, and also some singularities in orbital parameters may occur [8, 18]Control, . In [18], this assumption has been relaxed by introducing a specific orbital element-based parametrization of the relative dynamics. [18-20] applied LQR control in linearized orbital dynamics to minimize a predefined maneuver cost. However, in the presence of disturbances which is the definitive term of orbital dynamics in space missions and possible actuator faults, the performance of the closed loop system is decreased. Therefore, to have a precise and reliable maneuver even with the failure of the actuators and also to minimize fuel consumption, it is necessary to design an optimal fault-tolerant control.

In general, there are two approaches to designing a fault-tolerant controller; passive and active. In passive approaches, the controller is designed such that the closed loop system is robust to some expected faults, and the parameters and the structure of the controller do not change during the operation of the system [21-23]. While in active approaches, the parameters and controller structure are reconfigured based on the occurred fault. This approach can also be divided into two general categories. In the first category, there is not a unit for fault detection, isolation, and identification.

*Corresponding author's email: fa_jahangiri@sbu.ac.ir

However, this unit is required in the second category [24-26]. Although passive approaches require neither detection unit nor controller reconfiguration, they are only reliable for a predetermined class of faults and do not perform optimally for all fault scenarios.

An effective active fault tolerant control is the fault hiding method. The main idea of this method is to keep the nominal controller and design a block that is placed between the faulty process and the nominal controller such that the faults remain hidden from the nominal controller. In fact, this block is added to the faulty process so that the outputs and inputs of the augmented system (faulty process and the block) behave like a fault-free system. The main advantage of this approach is that there is no need to change the nominal controller and the block can be easily added to the existing nominal controller [25-27].

In this paper, the LQR control is augmented by terms such that the disturbances and actuator faults are estimated by a neural network and eliminated from the closed-loop system. In addition, model reference control is used to regulate the maneuvering error dynamics. As mentioned, most of the existing research used classical orbital parameters-based dynamics that can result in singularities. However, in this paper, we use modified orbital elements-based dynamics in the control design. The control command applies in Kepler orbital dynamics which is subject to disturbances and actuator faults by a Hall effect thruster since analysis of maneuvers shows that electric thrusters are suitable for satellite missions in LEO orbits to change phase and altitude [28]. Therefore, the contributions of this paper can be summarized as follows: 1) Modified orbital elements-based dynamics are used to design the controller. 2) Fault-tolerant LQR control is designed for orbital maneuvering that uses a neural network to estimate disturbances and actuator faults. 3) By a Hall effect thruster the control signal is applied to Kepler dynamics which is subjected to disturbances and actuator faults. 4) Ultimately boundedness of the maneuvering error dynamics is proved using Lyapunov analysis.

In section 2, Kepler's orbital dynamics of the satellite as well as modified orbital elements are discussed. In addition, the Hall effect thruster model is given. Section 3 proposes the fault-tolerant LQR which uses a neural network to eliminate the effects of disturbances and actuator fault. In this section, a theorem with its proof is given that guarantees the ultimately boundedness of the closed loop system. In section 4, simulation results are provided to demonstrate the effectiveness of the proposed method. Finally, section 5 concludes the paper.

2- Orbital Dynamics Based on Modified Elements

The equations of Kepler's orbit are the description of the movement of an object like a satellite in an orbit subjected to the gravitational force of another object. In addition, there are disturbance forces such as solar radiation pressure, atmospheric drag, earth gravity, third body, solar radiation, and the earth non-sphericity that affect the satellite movement. In general, taking into account all disturbances, the satellite orbital dynamics is as follows [8]:

$$\frac{d^2r}{dt^2}=\frac{-\mu}{\|r\|^3}r+\gamma_d+u_{ECI}, \tag{1}$$

where μ is the gravitational parameter of the earth, r provided the spacecraft position in Earth-Centered Inertial (*ECI*) coordinate, u_{ECI} is the *ECI* control acceleration, and γ_d denotes the environmental perturbation acceleration. The disturbances accelerations on the moving bodies around the earth change the orbital parameters.

The orbital motion is parameterized by the six orbital elements; a, e, i, Ω, ω, and ψ which are the semimajor axis, eccentricity, inclination, *RAAN*, argument of periapsis, and true anomaly (Figure 1). The parameters are expressed in *ECI* coordinates whose origin is located at the center of the earth. The second coordinate system is *RTN* which is in three directions; radial, tangential, and normal according to the right-hand rule. To avoid singularities, modified orbital elements are defined as follows [18]:

$$\begin{aligned}
x_1&=\Omega+\omega+\psi,\\
x_2&=\sqrt{\frac{\mu}{a^3}},\\
x_3&=e\cos(\Omega+\omega),\\
x_4&=e\sin(\Omega+\omega),\\
x_5&=\tan(\frac{i}{2})\cos(\Omega),\\
x_6&=\tan(\frac{i}{2})\sin(\Omega),
\end{aligned} \tag{2}$$

where x_1 is the true longitude, x_2 is the mean motion, (x_3, x_4) are the components of the eccentricity vector, (x_5, x_6) and are the components of the ascending node vector.

For maneuvering purposes, an error vector is defined between the modified orbital elements given by (2) and the reference orbital elements $x_i^*;\ \ i=1,2,\cdots,6$. The reference orbit is an ideal orbit that satisfies the mission aims and it is subjected to only the Earth's gravitational field force. Therefore, the errors are defined as [18]:

$$\begin{aligned}
\begin{bmatrix}\xi_3\\ \xi_4\end{bmatrix}&=\begin{bmatrix}\cos(x_1) & \sin(x_1)\\ \sin(x_1) & -\cos(x_1)\end{bmatrix}\begin{bmatrix}x_3-x_3^*\\ x_4-x_4^*\end{bmatrix},\\
\begin{bmatrix}\xi_5\\ \xi_6\end{bmatrix}&=\begin{bmatrix}\cos(x_1) & \sin(x_1)\\ \sin(x_1) & -\cos(x_1)\end{bmatrix}\begin{bmatrix}x_5-x_5^*\\ x_6-x_6^*\end{bmatrix}.
\end{aligned} \tag{3}$$

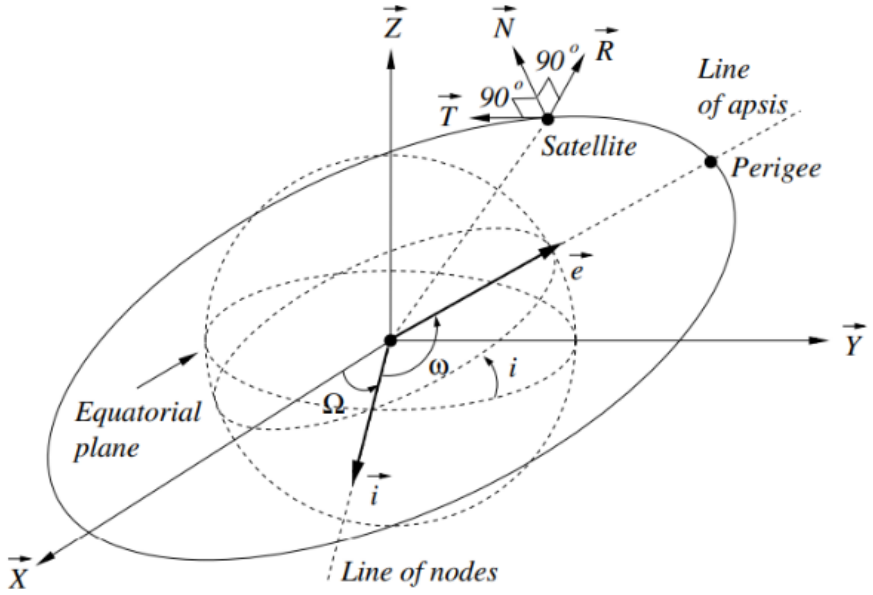

Fig. 1. Coordinate frames and orbit parameters [20]

Then, the error dynamics are described by [16]:

$$\frac{d\xi}{dt} = F\xi + Gu + \gamma_p, \tag{4}$$

where $u = [u_1 \quad u_2 \quad u_3]$ is the control input and it represents the acceleration vector in three radial, transverse, and normal directions in the *RTN* coordinate device. ξ is the state variables vector. During orbital transfers, only the error variables $\xi_2, \ldots, \xi_6$ are required to be controlled. Therefore, F and G are derived as follows:

$$F = \begin{bmatrix} 0 & 0 & 0 & 0 & 0 \\ 0 & 0 & \frac{(1+\zeta_3)^2 x_2}{-\omega^3 x_2^*} & 0 & 0 \\ 0 & \frac{(1+\zeta_3)^2 x_2}{\omega^3 x_2^*} & 0 & 0 & 0 \\ 0 & 0 & 0 & 0 & \frac{(1+\zeta_3)^2 x_2}{-\omega^3 x_2^*} \\ 0 & 0 & 0 & \frac{(1+\zeta_3)^2 x_2}{\omega^3 x_2^*} & 0 \end{bmatrix}, \tag{5}$$

$$G = \frac{\omega (x_2^*)^{1/3}}{\omega^* (x_2)^{1/3}} \begin{bmatrix} -\frac{3\zeta_4 x_2}{\omega^2 x_2^*} & -\frac{3(1+\zeta_3)x_2}{\omega^2 x_2^*} & 0 \\ 0 & 2 & 0 \\ 1 & \frac{\zeta_4}{1+\zeta_3} & 0 \\ 0 & 0 & \frac{1+\zeta_5^2-\zeta_6^2}{2(1+\zeta_3)} \\ 0 & 0 & \frac{\zeta_5\zeta_6}{1+\zeta_3} \end{bmatrix}, \tag{6}$$

where ω, ζ_3, ζ_4, ζ_5 and ζ_6 are defined as follows:

$$\omega = \sqrt{1 - x_3^2 - x_4^2},$$
$$\begin{bmatrix} \zeta_3 \\ \zeta_4 \end{bmatrix} = \begin{bmatrix} \cos(x_1) & \sin(x_1) \\ \sin(x_1) & -\cos(x_1) \end{bmatrix} \begin{bmatrix} x_3 \\ x_4 \end{bmatrix}, \tag{7}$$
$$\begin{bmatrix} \zeta_5 \\ \zeta_6 \end{bmatrix} = \begin{bmatrix} \cos(x_1) & \sin(x_1) \\ \sin(x_1) & -\cos(x_1) \end{bmatrix} \begin{bmatrix} x_5 \\ x_6 \end{bmatrix}.$$

$\gamma_p \in \mathbb{R}^{5\times1}$ is the total disturbances. The satellite is equipped with an electric thruster, Hall effect, for maneuvering control. The thrust provided by the Hall-effect thruster is obtained from the commanded thrust p_c, expressed in the inertial reference frame as follows [29]:

$$T = \Re(I_{3\times3} - \varepsilon_p)\begin{bmatrix}(1+f_p)p_c + \omega_p \\ 0 \\ 0\end{bmatrix}, \tag{8}$$

where I is identity matrix, $\Re \in \mathbb{R}^{3\times3}$ is conversion matrix of coordinate to *ECI*, $\varepsilon_p \in \mathbb{R}^{3\times3}$ is thrust alignment error, f_p is scale-factor bias and ω_p is actuator noise. An important parameter that describes the characteristics of the thrust source is the specific impulse, I_{sp}, which indicates the efficiency of converting fuel mass into thrust energy. The mass of consumed fuel is obtained from the following equation:

$$\dot{m} = \frac{T}{I_{sp}g}, \tag{9}$$

where g is the earth's gravitational constant.

3- Neural Network-based Fault Tolerant LQR Control

In this section, the orbital maneuvering control is designed to transfer from a primary LEO orbit to a secondary one. Quadratic linear optimal controller is a suitable choice for multi-input multi-output systems and has been used in many applications. However, the orbital elements of a satellite deviate from their desired values under the influence of disturbance forces. Therefore, the LQR controller is improved to overcome disturbances and faults. In control design, modified element dynamics are used to prevent singularities. Linearizing the nonlinear model (4) we have [8]:

$$\frac{d\xi}{dt} = A\xi + Bu + \gamma_p, \tag{10}$$

where the matrices A and B are:

$$A = \begin{bmatrix}0&0&0&0&0\\0&0&-1&0&0\\0&1&0&0&0\\0&0&0&0&-1\\0&0&0&1&0\end{bmatrix}, \quad B = \begin{bmatrix}0&-3&0\\0&2&0\\1&0&0\\0&0&0.5\\0&0&0\end{bmatrix}. \tag{11}$$

We consider the cost function to minimize fuel consumption and at the same time minimize orbital maneuvering error in the following form:

$$\min \int_0^\infty (\xi^T Q_1 \xi + u_c{}^T R_1 u_c)\, dt, \tag{12}$$

where $R_1 > 0$ and $Q_1 \geq 0$ are the weight matrices of inputs and maneuvering errors, respectively. Then, the state feedback control law is:

$$u_c = K\xi; \quad K = R_1^{-1} B^T R_1 P_1, \tag{13}$$

where P_1 is a positive definite matrix obtained from the following Riccati equation:

$$A^T P_1 + P_1 A - P_1 B R_1^{-1} B^T P_1 + Q_1 = 0. \tag{14}$$

Since the LQR is not able to eliminate the effects of disturbances and actuators faults, to improve the efficiency of the closed-loop system, we augment the LQR control with a block based on a neural network. The laws for updating the parameters are derived using Lyapunov analysis. The idea is that the nominal control (e.g. LQR) is designed for the nominal dynamics model that is free of disturbances and faults. Then, for the error dynamics between the nominal model and the model affected by disturbances and faults, the controller is modified such that the disturbances and faults are estimated using a neural network and then removed from the dynamics. In addition, a reference model is also designed for the desired efficiency of the error dynamics. In the proposed method, unlike most of the similar papers, the assumptions of knowing an upper bound for disturbances and their derivatives are not required.

The nominal dynamics without faults and disturbances are:

$$\begin{cases}\dot{\xi}(t) = A\xi(t) + Bu_c \\ y(t) = C\xi(t)\end{cases}, \tag{15}$$

where $u_c(t) \in \mathbb{R}^{3\times1}$ is the nominal LQR, $y \in \mathbb{R}^{l\times1}$ is the nominal dynamics output and $C \in \mathbb{R}^{l\times5}$ is a constant matrix.

Assumption 1: The closed loop system (15) by the designed LQR is stable with desired performance.

The system dynamics subject to disturbances and actuator faults are expressed by:

$$\begin{cases}\dot{\xi}_f(t) = A\xi_f(t) + B_f(u_f + f(t)) + \gamma_p(t); \quad \xi_f(0) = \xi_0, \\ y_f(t) = C\xi_f(t),\end{cases} \tag{16}$$

where $\xi_f(t) \in \mathbb{R}^{5\times1}$ is the state of the faulty dynamics, $y_f \in \mathbb{R}^{l\times1}$ is the faulty dynamics output and $u_f \in \mathbb{R}^{3\times1}$ is the faulty dynamics input. $f(t) \in \mathbb{R}^{3\times1}$ is the additive time-varying actuator fault. The loss of effectiveness actuator fault is formulated as the change in the input matrix [30]:

$B_f = B\Theta, \quad \Theta \triangleq diag(\theta_1, \theta_2, \theta_3),$

where $\theta_i;\ i = 1, 2, 3,$ are unknown constants such that $0 < \theta_i \le 1$. $\theta_i = 1$ means that the ith actuator is healthy. γ_p which is the total disturbances, written in two parts:

$\gamma_p(t) = Ed_1(t) + d_2(t).$

where $E \in \mathbb{R}^{5\times q}$, $d_1(t) \in \mathbb{R}^{q\times 1}$, $d_2(t) \in \mathbb{R}^{5\times 1}$. Satisfying the following assumption, unlike $d_2(t)$, the first part can be added to the control input u_f. Therefore, two different approaches are considered for $d_1(t)$ and $d_2(t)$ in control design that are discussed in following.

Assumption 2: The image space of E, $\mathrm{Im}(E)$, is a subspace of the image space of B, $\mathrm{Im}(B)$; $\mathrm{Im}(E) \subseteq \mathrm{Im}(B)$.

Since Θ is full rank, $\mathrm{Im}(B) = \mathrm{Im}(B_f)$ and there exists a matrix $Q^* \in \mathbb{R}^{3\times q}$ such that $B_f Q^* = E$.

Assumption 3: $d_2(t) \le \bar{d}_2$ where $\bar{d}_2$ is a constant vector.

The error dynamics between (15) and (16) are:

$$\begin{cases} \dot{\xi}_\Delta(t) = A\xi_\Delta(t) + B_f(u_f + d_t) + d_2(t) - Bu_c(t); \quad \xi_\Delta(0) = \xi_0, \\ y_\Delta(t) = C\xi_\Delta(t), \end{cases} \tag{17}$$

where $\xi_\Delta(t) \triangleq \xi_f(t) - \xi(t)$ and $d_t = f(t) + Q^* d_1(t)$. d_t is modeled by a one layer neural network with any desired accuracy as:

$$d_t(t) = W^*\phi(t) + \varepsilon(t), \tag{18}$$

where $W^* \in \mathbb{R}^{3\times k}$ is the weight matrix of the neural network and $\phi(.) \in \mathbb{R}^{k\times 1}$ is an activation function which is chosen as a sigmoid function. $\varepsilon(.) \in \mathbb{R}^{3\times 1}$ is the approximation error vector which from the universal approximation theorem [31], can be minimized as less as desired. We consider the upper bound $\bar{\varepsilon}$ as follows:

$$\|\varepsilon(t)\|_2 \le \bar{\varepsilon}. \tag{19}$$

Equation (18) is approximated by:

$$\hat{d}_t(t) = \hat{W}\phi(t), \tag{20}$$

where $\hat{W} \in \mathbb{R}^{3\times k}$ is the estimation of W^*. Therefore, the approximation error is defined as:

$$\tilde{d}_t(t) \triangleq \hat{d}_t(t) - d_t(t) = \left(\hat{W} - W^*\right)\phi(t) - \varepsilon(t). \tag{21}$$

The fault-tolerant control is designed as:

$$u_f(t) = M(t)\xi_\Delta(t) + N(t)u_c(t) - \hat{W}(t)\phi(t), \tag{22}$$

with the following updating laws for $\hat{W}(t)$, $N(t) \in \mathbb{R}^{3\times 3}$, and $M(t) \in \mathbb{R}^{3\times 5}$:

$$\dot{M}(t) = \mathrm{Proj}_{\mathrm{m}}\left[M(t), -B^T P\xi_\Delta(t)\xi_f^T(t)\right]\Gamma_M; \quad M(0) = M_0, \tag{23}$$

$$\dot{N}(t) = \mathrm{Proj}_{\mathrm{m}}\left[N(t), -B^T P\xi_\Delta(t)u_c^T(t)\right]\Gamma_N; \quad N(0) = N_0, \tag{24}$$

$$\dot{\hat{W}}(t) = \mathrm{Proj}_m\left[\hat{W}(t), B^T P\xi_\Delta(t)\varphi^T\right]\Gamma_{\hat{W}}; \quad \hat{W}(0) = \hat{W}_0, \tag{25}$$

where $\Gamma_M \in \mathbb{R}^{5\times 5}$, $\Gamma_N \in \mathbb{R}^{3\times 3}$, and $\Gamma_{\hat{W}} \in \mathbb{R}^{k\times k}$ are positive definite matrices that determine learning rates. The operator Proj_m of two matrices $X \in \mathbb{R}^{n\times m}$ and $Y \in \mathbb{R}^{n\times m}$ is defined as $\mathrm{Proj}_m(X,Y) = \left(\mathrm{Proj}\left(\mathrm{col}_1(X), \mathrm{col}_1(Y)\right), \ldots, \mathrm{Proj}\left(\mathrm{col}_m(X), \mathrm{col}_m(Y)\right)\right)$ where $\mathrm{col}_i(.)$ denotes the ith column, and the operator Proj of two vectors $x \in \mathbb{R}^{n\times 1}$ and $y \in \mathbb{R}^{n\times 1}$ is as follows:

$$\mathrm{Proj}(x,y) \triangleq \begin{cases} y, & \text{if } \phi(x) < 0, \\ y, & \text{if } \phi(x) \ge 0 \text{ and } \phi'(x)y \le 0, \\ y - \dfrac{\phi'^T(x)\phi'(x)y}{\phi'(x)\phi'^T(x)}\phi(x), & \text{if } \phi(x) \ge 0 \text{ and } \phi'(x)y > 0, \end{cases} \tag{26}$$

where $\phi(x) \triangleq \dfrac{(\varepsilon_x + 1)x^T x - x_{\max}^2}{\varepsilon_x x_{\max}^2}$, $\phi'(x) \triangleq \dfrac{\partial\phi(x)}{\partial x}$, $x_{\max} \in \mathbb{R}$ is a projection norm bound imposed on x, and $\varepsilon_x > 0$ is a projection tolerance bound. It can be shown that [32]:

$$(x - x^*)^T(\mathrm{Proj}(x,y) - y) \le 0, \quad x^* \in \mathbb{R}^n, \quad \phi(x^*) \le 0. \tag{27}$$

Therefore, from (27), for any $X \in \mathbb{R}^{n\times m}$ we have:

$$\begin{aligned} &tr\left[(X - X^*)^T(\mathrm{Proj}_m(X,Y) - Y)\right] \\ &= \sum_{i=1}^{m}\left[\mathrm{col}_i(X - X^*)^T(\mathrm{Proj}(\mathrm{col}_i(X), \mathrm{col}_i(Y)) - \mathrm{col}_i(Y))\right] \le 0. \end{aligned} \tag{28}$$

The matrix $P \in \mathbb{R}^{5\times 5}$ is obtained from the following Lyapunov equation:

$$A_d^T P + PA_d + Q = 0, \tag{29}$$

where $Q \in \mathbb{R}^{5\times 5}$ is a positive matrix and $A_d \in \mathbb{R}^{5\times 5}$ is a Hurwitz matrix which determines the desired performance of the error dynamics.

Assumption 4: There exists matrices $N^* \in \mathbb{R}^{3\times 3}$, and $M^* \in \mathbb{R}^{3\times 5}$ such that:

$$B_f N^* - B = 0, \quad A + B_f M^* = A_d. \tag{30}$$

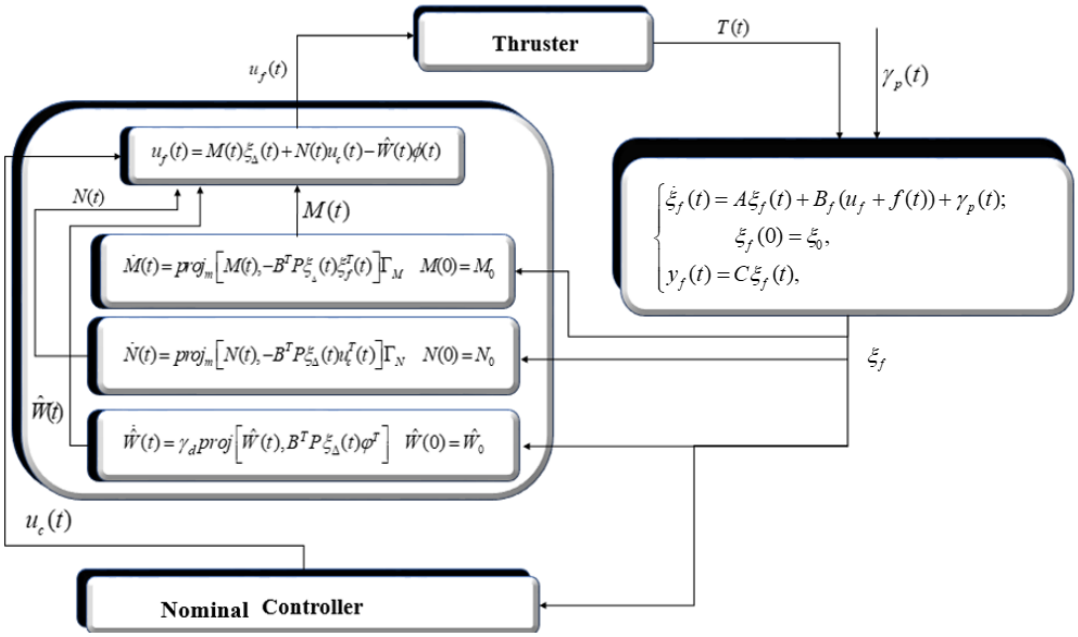

Fig. 2. Control structure to eliminate the effect of disturbances and faults

Figure 2 shows the block diagram of the closed-loop system with the proposed controller and the updating laws.

Theorem 1: Consider the error dynamics given by (17) with control input (22) and updating laws (23) - (25). If Assumptions 1 to 4 are satisfied then $\xi_\Delta(t)$ is ultimately bounded with ultimate bound as:

$$\mu=\frac{2\lambda_{\max}(P)\left(\|B\|\bar{\varepsilon}+\bar{d}_2\right)}{\lambda_{\min}(Q)}. \tag{31}$$

Proof: The dynamics of orbital maneuvering error (17) which is affected by disturbances and faults, and by the proposed control law (22) is as follows:

$$\begin{aligned}&\dot{\xi}_\Delta(t)=A\xi_\Delta(t)+B_fM(t)\xi_\Delta(t)+\\&B_fN(t)u_c(t)+B_f(d_t(t)-\hat{W}(t)\varphi(t))+\\&d_2(t)-Bu_c(t)\\&=A\xi_\Delta(t)+B_f(M^*+M(t)-M^*)\xi_\Delta(t)+\\&B_f(N^*+N(t)-N^*)u_c(t)+B_f(d_t(t)-\\&\hat{W}(t)\varphi(t))+d_2(t)-Bu_c(t)\\&=(A+B_fM^*)\xi_\Delta(t)+B_f\tilde{M}\xi_\Delta(t)+B_f\tilde{N}u_c(t)-\\&B_f\tilde{d}_t(t)+(B_fN^*-B)u_c(t)+d_2(t),\end{aligned} \tag{32}$$

where $\tilde{M}(t)\triangleq M(t)-M^*$, $\tilde{N}(t)\triangleq N(t)-N^*$, and $\tilde{d}_t(t)\triangleq\hat{d}_t(t)-d_t(t)$. Using Assumption 4 the dynamics (32) is written as:

$$\dot{\xi}_\Delta(t)=A_d\xi_\Delta(t)+B_f\tilde{M}\xi_\Delta(t)+B_f\tilde{N}u_c(t)-B_f\tilde{d}_t(t)+d_2(t). \tag{33}$$

In addition, since the weights updates $M(t)$, $N(t)$, and $\hat{d}_t(t)$ are calculated from Proj operator, there exist norm bounds $\tilde{M}_{\max}$, $\tilde{N}_{\max}$, and $\tilde{d}_{t,Max}$ such that $\|\tilde{M}(t)\|_F\le\tilde{M}_{\max}$, $\|\tilde{N}(t)\|_F\le\tilde{N}_{\max}$, and $\|\tilde{d}_t(t)\|_2\le\tilde{d}_{t,Max}$ for $t\ge0$. The Lyapunov function is chosen as follows:

$$\begin{aligned}&V(\xi_\Delta(t),\tilde{M}(t),\tilde{N}(t),\tilde{W}(t))\\&=\xi_\Delta^T(t)P\xi_\Delta(t)+tr\left\{\Gamma_M^{-1}\tilde{M}^T(t)N^{*-1}\tilde{M}(t)\right\}\\&+tr\left\{\Gamma_N^{-1}\tilde{N}^T(t)N^{*-1}\tilde{N}(t)\right\}+\eta_d^{-1}\,trace\left\{\tilde{W}^TN^{*-1}\tilde{W}\right\}.\end{aligned} \tag{34}$$

where $\tilde{W}(t)\triangleq W(t)-W^*$. The derivative of $V(\xi_\Delta(t),\tilde{M}(t),\tilde{N}(t),\tilde{W}(t))$ along the trajectory (33), and using (23), (24), and (29) we have:

$$\begin{aligned}&\dot{V}(\xi_\Delta(t),\tilde{M}(t),\tilde{N}(t),\tilde{W}(t))\\&=-\xi_\Delta^T(t)Q\xi_\Delta(t)+2\xi_\Delta^T(t)PB_f\tilde{M}(t)\xi_\Delta(t)\\&+2\xi_\Delta^T(t)PB_f\tilde{N}(t)u_c(t)-2\xi_\Delta^T(t)PB_f\tilde{d}_t(t)\\&+2tr\left\{\tilde{M}(t)\,\mathrm{Proj}_m\left[M(t),-B^TP\xi_\Delta(t)\xi_\Delta^T(t)\right]\right\}\\&+2tr\left\{\tilde{N}^T(t)\,\mathrm{Proj}_m\left[N(t),-B^TP\xi_\Delta(t)u_c^T(t)\right]\right\}\\&+2d_2^T(t)P\xi_\Delta(t)+2\eta_d^{-1}trace\left\{\dot{\tilde{W}}^TN^{*-1}\tilde{W}(t)\right\}.\end{aligned} \tag{35}$$

Table 1. Orbits elements for the maneuvering scenario

Elements	Initial orbit	Final orbit
$a\,(Km)$	450	1000
i (deg)	82	81
e	0	0
ω (deg)	free	free
Ω (deg)	free	free
θ (deg)	free	free

Table 2. The perturbations characteristics

Earth gravitational constant	$\mu = 398600.47$
Acceleration of gravity	$g_0 = 9.81$
Effective cross-sectional of the satellite	$S = 0.5625$
Air density	$\rho = 7.388$
Earth radios	$R_e = 6378.1363$
Disturbance constant	$J_2 = 0.00108263$
Drag coefficient	$C_D = 2.5$

Using the property (28), for equation (35) we have:

$$\dot{V} \le -\xi_\Delta^T(t)Q\xi_\Delta(t) + 2d_2^T(t)P\xi_\Delta(t) - 2\xi_\Delta^T(t)PB_f\tilde{d}_t(t) + 2\eta_d^{-1}trace\left\{\dot{\tilde{W}}^T N^{*-1}\tilde{W}(t)\right\}. \quad (36)$$

By equation (21), the relation (36) is written as:

$$\dot{V} \le -\xi_\Delta^T(t)Q\xi_\Delta(t) + 2d_2^T(t)P\xi_\Delta(t) - 2\xi_\Delta^T(t)PB_f\tilde{W}(t)\varphi(t) - 2\xi_\Delta^T(t)PB_f\varepsilon(t) + 2\eta_d^{-1}trace\left\{\dot{\tilde{W}}^T N^{*-1}\tilde{W}(t)\right\}, \quad (37)$$

Now substituting (25) and using the property (28), we have:

$$\dot{V} \le -\xi_\Delta^T(t)Q\xi_\Delta(t) + 2d_2^T(t)P\xi_\Delta(t) - 2\xi_\Delta^T(t)PB_f\varepsilon(t), \quad (38)$$

where from 19 and also Assumption 3, it is written as:

$$\dot{V} \le -\lambda_{\min}(Q)\|\xi_\Delta(t)\|^2 + 2\|\xi_\Delta(t)\|\lambda_{\max}(P)\left(\|B\|\bar{\varepsilon} + \bar{d}_2\right). \quad (39)$$

$\lambda_{\min}(Q)$ and $\lambda_{\max}(P)$ are the minimum and maximum eigenvalues of the matrices Q and P, respectively. Now, it is obvious that the condition for the right side of (39) to become negative is $\|\xi_\Delta(t)\| \ge 2\lambda_{\max}(P)\left(\|B\|\bar{\varepsilon} + \bar{d}_2\right)/\lambda_{\min}(Q)$. Therefore, $\dot{V}(\xi_\Delta(t), \tilde{M}(t), \tilde{N}(t), \tilde{W}(t)) < 0$, out of the region $\|\xi_\Delta(t)\| \ge \mu$, and ultimately boundedness of $\xi_\Delta(t)$ is proved

Remark 1. This theorem shows that by using the proposed control in the faulty dynamics (16), this dynamics has a behavior close to the nominal dynamics (15), and therefore, due to Assumption 1, we can expect the desired performance from the closed loop faulty dynamics.

4- Simulation and Results

In this part, the proposed controller is used to transfer the satellite between two LEO orbits and compare it with LQR. The initial and final conditions for the desired mission are given in Table 1. As mentioned earlier, during the transfer of the orbit, the three elements of height, eccentricity, and inclination of the orbit change. Since the three elements Ω, ω, and θ, which are of the angle type, do not affect the transfer of the orbit, they are considered free. In addition, the orbit transfer mission is from 450 km altitude to 1000 km altitude by considering the radius of the earth which is 6371 km, the altitude should be transferred from 6821 km to 7371 km.

The orbit dynamics are subject to the disturbances; earth gravity, atmospheric drag, third body and solar radiation with the characteristics given in Table 2.

Table 3. Thruster parameters

Earth gravitational constant	$\mu = 398600.47$
Acceleration of gravity	$g_0 = 9.81$
Effective cross-sectional of the satellite	$S = 0.5625$
Air density	$\rho = 7.388$
Earth radios	$R_e = 6378.1363$
Disturbance constant	$J_2 = 0.00108263$
Drag coefficient	$C_D = 2.5$

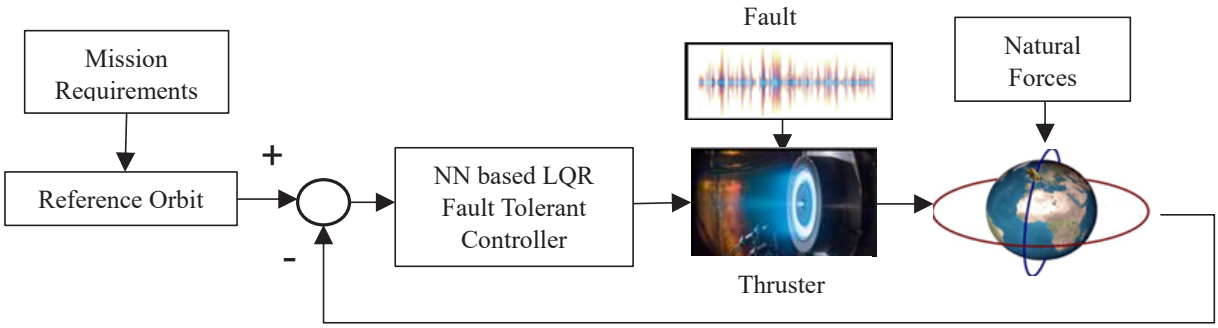

Fig. 3. Block diagram of orbital maneuvering control

The actuator is a Hall effect thruster with a limited thrust 15 mN and the parameters are given in Table 3. The value of the additive actuator fault is considered as follows for times between the days 26th and 38th:

$$f(t) = \begin{bmatrix} 0.001\sin(0.05t) & 0 & 0 \end{bmatrix}^T .$$

We apply the proposed controller to the nonlinear kepler model with deterministic model of disturbances includes earth gravity, atmospheric drag, third body and solar radiation from the model [33] as well as the actuator faults. The block diagram of orbital maneuvering control using neural network based fault tolerant LQR controller and Hall effect thruster is shown in Figure 3.

The simulation results including altitude, eccentricity, and orbit inclination for 50 days are shown in Figure 4. As seen, by the proposed fault tolerant control method, in addition of meeting the maneuvering mission specifications, the effects of disturbances and faults vanished. Figure 5 shows the thruster signal which satisfies its limitation. To show the effectiveness of the proposed method, the simulation is repeated by LQR controller. The results for the three orbital elements altitude, eccentricity, and inclination are shown in Figure 6. In order to check the performance of the closed-loop system more closely, the results are zoomed in Figure 7. It is seen that the three elements have unfavorable fluctuations due to the existence of disturbances and the fault. For example, the altitude element has about 10 kilometers of fluctuation due to the disturbances and about 70 kilometers due to the fault. Therefore, comparing the results in Figures 6 and 7 with Figure 4, the proposed controller has higher performance than LQR in the presence of the disturbances and faults, since in the proposed method, a possible part of disturbances and also faults are estimated by the neural network which is augment to the controller and then the effects of them are eliminated from the closed loop dynamics.

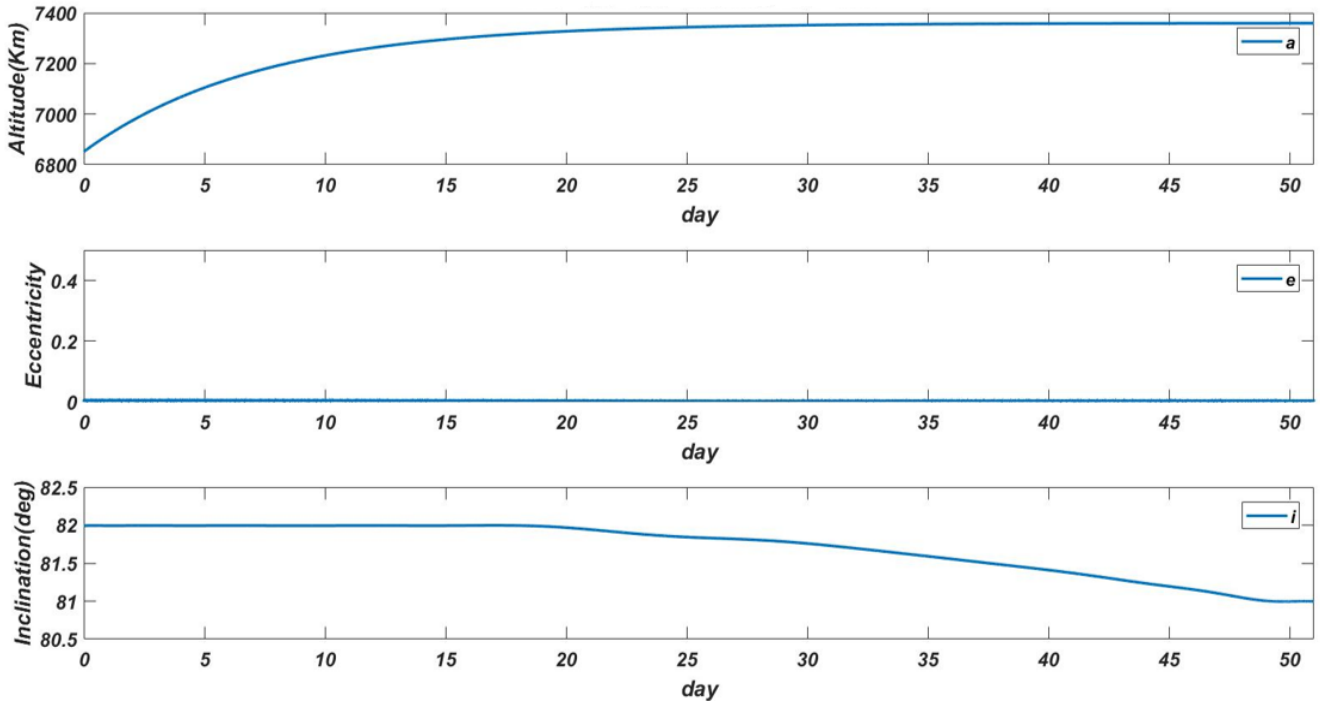

Fig. 4. Orbit elements during maneuvering by the proposed controller

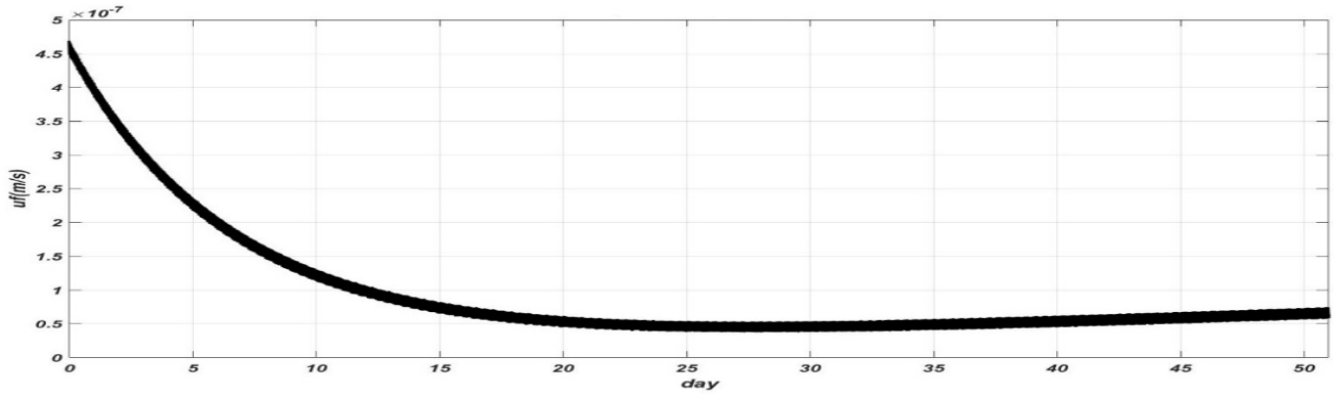

Fig. 5. Thruster signal

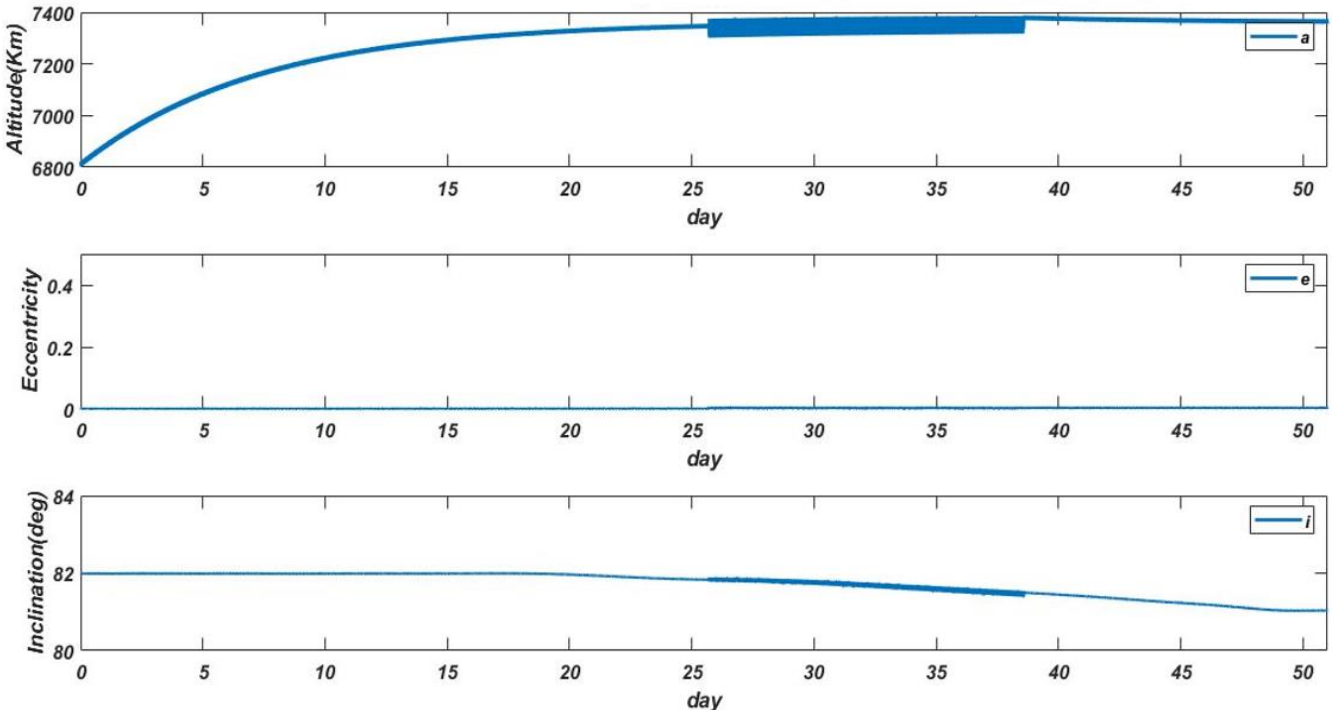

Fig. 6. Orbit elements during maneuvering by LQR

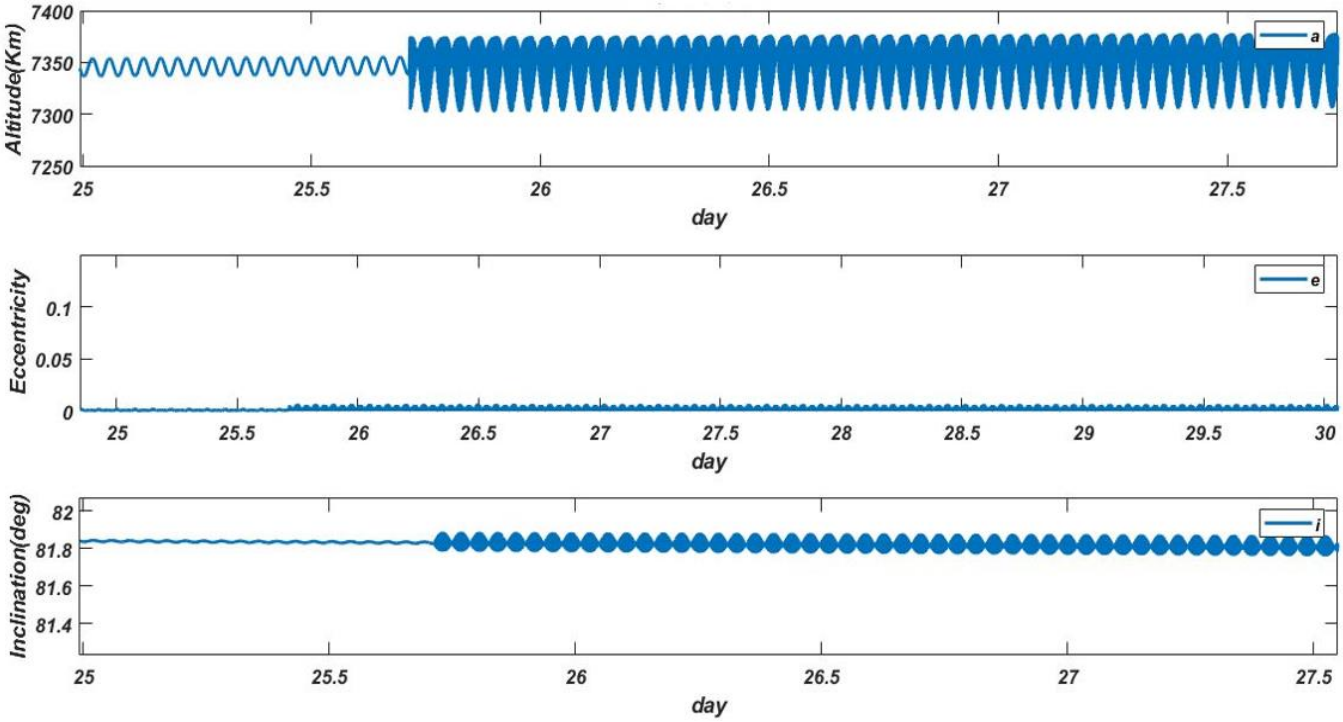

Fig. 7. Zoomed orbit elements during maneuvering by LQR

5- Conclusion

In this paper, a neural network-based fault tolerant LQR control has been designed for the purpose of orbit maneuvering between two LEO orbits. To avoid singularities, the orbital dynamics based on the modified elements were used. The dynamics were considered to be subjected to disturbances; earth gravity, atmospheric drag, third body and solar radiation, and also thruster faults. The reference orbit is the orbital dynamics which is subjected to only the gravity acceleration. Hall effect thrusters were used as the actuator due to their high performance and are widely used in LEO satellites. Ultimately boundedness of the maneuvering error has been proved by Lyapunov analysis. The designed controller was applied in nonlinear Kepler orbit dynamics which is affected from an accurate model of natural disturbances. The simulation results show the high performance of the closed-loop system with the proposed controller.

References

[1] D. A. Vallado, Fundamentals of Astrodynamics and Applications, 3rd Edition ed. New York: Springer-Verlag, 2007.

[2] J. A. Starek, B. Açıkmeşe, I. A. Nesnas, and M. Pavone, "Spacecraft Autonomy Challenges for Next-Generation Space Missions," in Advances in Control System Technology for Aerospace Applications, E. Feron Ed. Berlin, Heidelberg: Springer Berlin Heidelberg, 2016, pp. 1-48.

[3] M. Leomanni, A. Garulli, A. Giannitrapani, and F. Scortecci, "Propulsion options for very low Earth orbit microsatellites," Acta Astronautica, vol. 133, pp. 444-454, 2017.

[4] C. M. Kellett and L. Praly, "Nonlinear control tools for low thrust orbital transfer," IFAC Proceedings Volumes, vol. 37, no. 13, pp. 79-86, 2004.

[5] P. Singla, K. Subbarao, and J. L. Junkins, "Adaptive Output Feedback Control for Spacecraft Rendezvous and Docking Under Measurement Uncertainty," Journal of Guidance, Control, and Dynamics, vol. 29, no. 4, pp. 892-902, 2006.

[6] M. Leomanni, G. Bianchini, A. Garulli, and A. Giannitrapani, "A class of globally stabilizing feedback controllers for the orbital rendezvous problem," International Journal of Robust and Nonlinear Control, vol. 27, pp. 4296-4311, 2017.

[7] L. Steindorf, S. D'Amico, J. Scharnagl, F. Kempf, and K. Schilling, "Constrained Low-Thrust Satellite Formation-Flying Using Relative Orbit Elements," presented at the 27th AAS/AIAA Space Flight Mechanics Meeting, AAS Paper, 2017.

[8] M. Leomanni, G. Bianchini, A. Garulli, A. Giannitrapani, and R. Quartullo, "Orbit Control Techniques for Space Debris Removal Missions Using Electric Propulsion," Journal of Guidance, Control, and Dynamics, vol. 43, pp. 1-10, 2020.

[9] Y. Wang, C. Han, and X. Sun, "Optimization of low-thrust Earth-orbit transfers using the vectorial orbital elements," Aerospace Science and Technology, vol. 112, 2021.

[10] R. Fuhr and A. Rao, "Minimum-Fuel Low-Earth-Orbit Aeroglide and Aerothrust Aeroassisted Orbital Transfer Subject to Heating Constraints," Journal of Spacecraft and Rockets, vol. 55, pp. 1-26, 2018.

[11] S. Huang, C. Colombo, and F. Bernelli-Zazzera, "Low-thrust Planar Transfer for Co-Planar Low Earth Orbit Satellites Considering Self-Induced Collision Avoidance," Aerospace Science and Technology, 2020.

[12] L. Zhang, B. Xu, M. Li, and F. Zhang, "Semi-analytical approach for computing near-optimal low-thrust transfers to geosynchronous orbit," Aerospace Science and Technology, vol. 55, pp. 482-493, 2016.

[13] H. Shen, S. Xue, and D. Li, "MPC-based Low-thrust Orbit Transfer Under J 2 Perturbation," in 2020 39th Chinese Control Conference (CCC), 2020: IEEE, pp. 2467-2472.

[14] R. Chai, A. Savvaris, A. Tsourdos, S. Chai, and Y. Xia, "Optimal tracking guidance for aeroassisted spacecraft reconnaissance mission based on receding horizon control," IEEE Transactions on Aerospace and Electronic Systems, vol. 54, no. 4, pp. 1575-1588, 2018.

[15] W. Yu, Z. Penglei, and W. Chen, "Analytical Solutions to Aeroassisted Orbital Transfer Problem," IEEE Transactions on Aerospace and Electronic Systems, vol. 56, pp. 3502-3515, 2020.

[16] J. A. Starek and I. V. Kolmanovsky, "Nonlinear model predictive control strategy for low thrust spacecraft missions," Optimal Control Applications and Methods, vol. 35, no. 1, pp. 1-20, 2014.

[17] F. de Bruijn, E. Gill, and J. How, "Comparative analysis of Cartesian and curvilinear Clohessy-Wiltshire equations," Journal of Aerospace Engineering, Sciences and Applications, vol. 3, pp. 1-15, 2011.

[18] M. Leomanni, G. Bianchini, A. Garulli, and A. Giannitrapani, "State feedback control in equinoctial variables for orbit phasing applications," Journal of Guidance, Control, and Dynamics, vol. 41, no. 8, pp. 1815-1822, 2018.

[19] C. A. Kluever, "Comet Rendezvous Mission Design Using Solar Electric Propulsion Spacecraft," Journal of Spacecraft and Rockets, vol. 37, no. 5, pp. 698-700, 2000.

[20] D. Losa, M. Lovera, R. Drai, T. Dargent, and J. Amalric, "Electric Station Keeping of Geostationary Satellites: a Differential Inclusion Approach," presented at the 44th IEEE Conference on Decision and Control, Seville, Spain, 2006.

[21] S. Raval, H. R. Patel, S. Patel, and V. A. Shah, "Passive Fault-Tolerant Control Scheme for Nonlinear Level Control System with Parameter Uncertainty and Actuator Fault," in Applications of Fuzzy Techniques, Cham, 2023: Springer International Publishing, pp. 229-242.

[22] M. A. Zuñiga, L. A. Ramírez, G. Romero, E. Alcorta-García, and A. Arceo, "Passive Fault-Tolerant Control of a 2-DOF Robotic Helicopter," Information, vol. 12, no. 11, 2021.

[23] A. Shamisa and Z. Kiani, "Robust fault-tolerant controller design for aerodynamic load simulator," Aerospace Science and Technology, vol. 78, pp. 332-341,

2018.

[24] A. Abbaspour, S. Mokhtari, A. Sargolzaei, and K. K. Yen, "A Survey on Active Fault-Tolerant Control Systems," Electronics, vol. 9, no. 9, 2020.

[25] J. Cieslak and D. Henry, "A Switching Fault-Hiding Mechanism based on Virtual Actuators and Dwell-Time Conditions," IFAC-PapersOnLine, vol. 51, no. 24, pp. 703-708, 2018.

[26] I. Tahiri, A. Philippot, V. Carré-Ménétrier, and A. Tajer, "A Fault-Tolerant and a Reconfigurable Control Framework: Application to a Real Manufacturing System," Processes, vol. 10, no. 7, 2022.

[27] M. Yadegar, N. Meskin, and A. Afshar, "Fault-tolerant control of linear systems using adaptive virtual actuator," International Journal of Control, vol. 92, no. 8, pp. 1729-1741, 2019.

[28] S. King, M. Walker, and C. Kluever, "Small Satellite LEO Maneuvers with Low-Power Electric Propulsion," presented at the 44th AIAA/ASME/SAE/ASEE Joint Propulsion Conference & Exhibit, 2008.

[29] A. Garulli, A. Giannitrapani, M. Leomanni, and F. Scortecci, "Autonomous low-Earth-orbit station-keeping with electric propulsion," Journal of guidance, control, and dynamics, vol. 34, no. 6, pp. 1683-1693, 2011.

[30] J. H. Richter, Reconfigurable Control of Nonlinear Dynamical Systems. Springer Berlin, Heidelberg, 2011.

[31] K. Hornik, M. Stinchcombe, and H. White, "Multilayer feedforward networks are universal approximators," Neural Networks, vol. 2, no. 5, pp. 359-366, 1989.

[32] Eugene Lavretsky and K. A. Wise, "Robust and Adaptive Control With Aerospace Applications," 2 ed: Springer Cham, 2013.

[33] J. R. Wertz, Spacecraft Attitude Determination and Control. Springer Dordrecht, 2012.

HOW TO CITE THIS ARTICLE

E. Jahanbazi goujani, F. Jahangiri, M. R. Mohammadi Damabi, Neural Network based Fault Tolerant LQR Control for Orbital Maneuvering in LEO Satellites using Hall Effect Thrusters. AUT J. Model. Simul., 55(1) (2023) 171-182.

DOI: 10.22060/miscj.2023.22482.5326